X-ray photoemission spectroscopy studies of cerium thin films on transition-metal foils: Ce/Re, Ce/Ir, and Ce/Pt

J. Tang and J. M. Lawrence
Institute for Surface and Interface Science and Department of Physics, University of California, Irvine, California 92717

J. C. Hemminger
Institute for Surface and Interface Science and Department of Chemistry, University of California, Irvine, California 92717
(Received 30 November 1992)

We report x-ray photoemission spectroscopy studies of the growth of ultrathin (0.1–5 monolayers) cerium films on polycrystalline rhenium, iridium, and platinum substrates. Our data indicate that Ce grows on Re without intermixing or compound formation, that on Pt reaction (i.e., compound formation) as well as interdiffusion is strong, while on Ir compound formation occurs but interdiffusion is weaker than for Pt. At low coverages the Ce has identical 3*d* binding energy and is trivalent for all three substrates and there appears to be a threshold for the onset of mixed-valence behavior.

I. INTRODUCTION

While studies of cerium thin films on transition-metal (M) substrates are fairly recent, interesting growth phenomena have already been reported. As is true for other rare earth (R) metals, epitaxial growth of elemental cerium films has been observed on refractory metal substrates (where no R_mM_n intermetallics form in the bulk) such as V or W.[1,2] Homma, Yang, and Schuller reported in Ref. 1 that a metastable phase of Ce forms films at least 50-Å thick on V(110). In this phase the Ce lattice has an 8% in-plane contraction and a 2% out-of-plane expansion with respect to γ-cerium, and furthermore the relative orientation of Ce(111) and V(110) planes is different from either the Kurdjumov-Sachs or Nisiyama-Wassermann orientations for epitaxial growth systems. In the Ce/W system, Gu *et al.* have shown, using valence-band photoemission spectra, that a γ-α phase transition occurs within the submonolayer range where the lattice constant changes from a value 9% larger than that of γ-cerium to a value 3% less than that of α-cerium.

When deposited on reactive substrates where bulk intermetallics are known to form, e.g., Cu,[3] Si,[4–6] Al,[7] and Au,[8] Ce reacts and forms interdiffusion layers with the substrates. The interdiffusion layers can be as much as 100-Å thick, and the formation of the mixed layers depends on properties such as diffusion rates, surface energy, and the heat of interface compound or alloy formation.[9] The onset of interdiffusion can also be very different; for example, in the Ce/Si(110) system[4,5] there is a critical coverage of 0.6 monolayers (ML) for the interdiffusion to happen, while there is no critical coverage observed in the Ce/Si(100) system.[6] Most of the work on reactive substrates has been done on polycrystalline foils and has focused on coverages substantially greater than 1 ML.

In this work we report studies of Ce films on polycrystalline 5*d* M substrates (Re, Ir, and Pt) where Ce film growth has not been studied in the past. We emphasize the low coverage regime, from submonolayer to a small number of overlayers. Re, which forms no bulk intermetallics with Ce,[10] should be a refractory substrate. Ir and Pt should be reactive because they are known to form compounds with Ce. Some of these compounds are mixed valent and thus a second emphasis is on the valence and its dependence on coverage and heat treatment. To this end we follow the well-established procedure[11,12] of using Ce 3*d* core levels to determine the valence. We use both the Ce 3*d* and M 4*f* core-level binding-energy shifts to characterize film growth and we show that changes in the Ce valence can be useful for the same end.

II. EXPERIMENTAL DETAILS

Experiments were performed at room temperature in a VG ESCALAB MKII chamber with base pressure of 6×10^{-11} mbar and operating pressure of 1×10^{-10} mbar. An aluminum $K\alpha$ x-ray source and a hemispherical analyzer were used; the overall x-ray photoemission spectroscopy (XPS) resolution was 1 eV.

Ir and Pt substrates were first bombarded with argon ions for 2 h at 800 °C, and then oxygen treated at 500 °C. Following this, the substrate was flashed to 1100 °C to expel CO and oxygen. Re substrates were first rough cleaned by ion bombardment at 800 °C for 4 to 5 h, and then exposed to hydrogen at 1000 °C to remove oxygen. After the hydrogen treatment, we heated the substrate to 1100 °C to remove the residual hydrogen. In the above cleaning procedures, resistive heating was used and the substrate holder and its environment were all previously degassed so that the pressure remained better than 6×10^{-10} mbar during flashing; the chamber returned to base pressure very rapidly. All substrates were checked by XPS after cleaning. Cerium was evaporated in a tungsten basket and the whole evaporation apparatus was carefully degassed before experiments. The pressure during evaporation never exceeded 1.5×10^{-10} mbar. In or-

0163-1829/93/47(24)/16477(9)/$06.00

der to avoid accumulated contamination, we bombarded Ce off the substrate after spectra for each coverage had been taken, rather than evaporating Ce successively.[6] Samples were annealed in successive 2 min cycles at 900 °C.

Cerium coverages were estimated by use of a nonreactive layer-by-layer model.[13] For Ce coverage ϑ in the submonolayer range, we have used the following expressions for Ce and substrate XPS count rates:

$$I_{\mathrm{Ce}}=\vartheta I^{0}_{\mathrm{Ce}}\left[1-\exp\left[-\frac{a}{\lambda_{\mathrm{Ce}}\cos\alpha}\right]\right], \tag{1}$$

$$I_{\mathrm{sub}}=\vartheta I^{0}_{\mathrm{sub}}\exp\left[-\frac{a}{\lambda_{\mathrm{sub}}\cos\alpha}\right]+(1-\vartheta)I^{0}_{\mathrm{sub}}\ . \tag{2}$$

For coverages above one monolayer, we used the following equations to determine the thickness x:

$$I_{\mathrm{Ce}}=I^{0}_{\mathrm{Ce}}\left[1-\exp\left[-\frac{x}{\lambda_{\mathrm{Ce}}\cos\alpha}\right]\right], \tag{3}$$

$$I_{\mathrm{sub}}=I^{0}_{\mathrm{sub}}\exp\left[-\frac{x}{\lambda_{\mathrm{sub}}\cos\alpha}\right]\ . \tag{4}$$

Here, I_{Ce} and I_{sub} are the measured count rates. I^{0}_{Ce} and I^{0}_{sub} are the respective count rates for the pure substances obtained under the same photoemission conditions (position, take-off angle, x-ray intensity, etc.), and they correspond to modified sensitivity factors. I^{0}_{Ce} for the Ce $3d_{5/2}$ level is 8.6, and the values of I^{0}_{sub} for the Re, Ir, and Pt $4f_{7/2}$ levels are 4.2, 3.0, and 3.4, respectively.[14] λ_{Ce} and λ_{sub} are the core-level photoelectron mean free paths; for Ce this was taken to be 12 Å, and for the three M substrates it was taken to be 15 Å.[15] The factor $\cos\alpha$ was taken to be unity for normal emission. In Eqs. (1) and (2), ϑ is the unknown coverage, and a is the Ce monolayer thickness which was estimated to be 3 Å. In Eqs. (3) and (4), x is the unknown thickness. In submonolayer cases, we divide Eq. (1) by Eq. (2) and solve for ϑ, while in overlayer cases, we divide Eq. (3) by Eq. (4) and solve for x.

Use of such models is obviously incorrect for the case

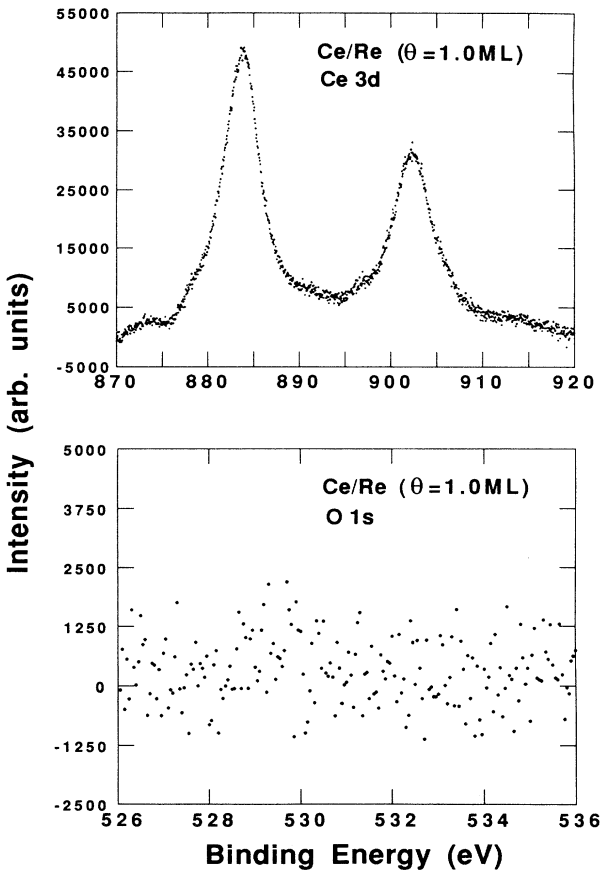

FIG. 1. Upper panel: Ce 3d region at 1-ML coverage in the Ce/Re system. Lower panel: Oxygen 1s region for this coverage. The contamination level is less than 2% of a monolayer. While the units for intensity are arbitrary, they are the same for both panels to facilitate comparison; the background emission has been substracted in each case.

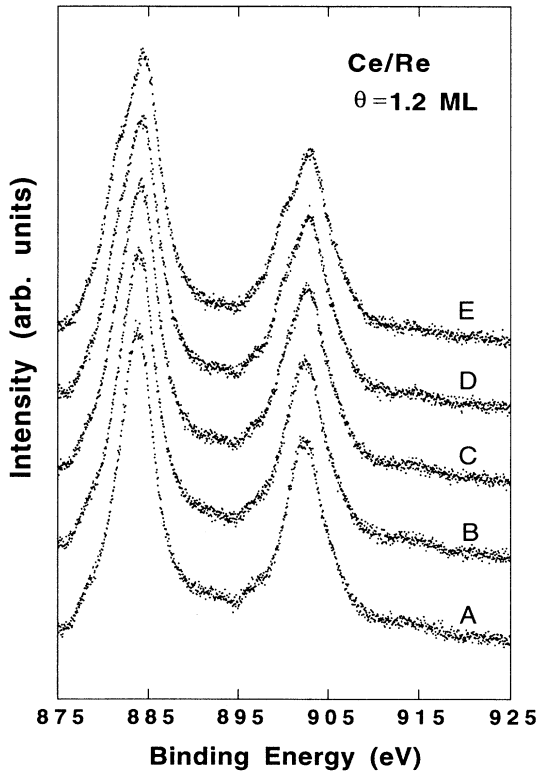

FIG. 2. Effect of oxygen contamination on the Ce 3d line shapes and binding energies at 1.2-ML Ce coverage in the Ce/Re system. Contaminants were obtained by simply letting the sample sit in the chamber for a long period of time. Spectra were taken roughly every 40 min. The corresponding oxygen contents are the following: A: 3% of a monolayer contamination; B: 10.2%; C: 11.4%; D: 18%; E: 21.6%. The Ce $3d4f^{1}$ binding energies shifted from 883.7 and 902.3 eV in A to 884.7 and 903.2 eV in E. The growth of the shoulders on the lower binding-energy side is obvious.

of interdiffusion or island formation. The difficulty is compounded for polycrystalline substrates due to differing surface orientations and grain boundaries. However, in a system where amorphous interdiffusion occurs and the detailed stoichiometry is unknown, rigorous calculation and calibration of coverage and structure are not possible. For reactive and interdiffused systems the number of Ce layers obtained from this model should be smaller than the actual Ce amount. This is due to the increased substrate count rate in an interdiffused system. At low coverages there is some hope that these formulas give correct values for coverage, especially if a threshold for reaction and/or diffusion exists. Otherwise the stated coverages are qualitative.

In Fig. 1, Ce $3d$ and O $1s$ spectra for Ce/Re are shown as an example of cleanliness. Using peak area ratios, we have determined that the contamination level was less than 3% of a monolayer. We have performed studies of the effect of oxygen contamination on both the line shapes and binding energies in the Ce $3d$ region. Representative spectra for the case Ce/Re are shown in Fig. 2; it can be seen that oxidation shifts the binding energies of the Ce $3d$ ($4f^1$ final state) features to higher values, and gives rise to visible shoulders.[16] As oxidation continues, the line shape eventually resembles that of Ce_2O_3.[17] Assuming that linear extrapolation yields a clean spectrum, we found that freshly deposited films (with oxygen contamination less than 3% of a monolayer) are very close to the ideal clean spectrum, but that spectra taken 30 min after evaporation already show visible contamination. The results reported below are for freshly evaporated films, and we are confident that they are not affected by such contamination.

III. RESULTS AND ANALYSIS

We have performed iterative background subtraction on all the data presented herein.[18] The binding energies given below were obtained by fitting the spectra to a sum of several Lorentzians.

Figure 3 shows XPS spectra of the Ce $3d$ region in both γ-cerium (our work) and $CeIr_2$.[16] In both curves, $4f^0$, $4f^1$, and $4f^2$ final-state features are indicated. It is clear that Ce $4f^0$ and $4f^2$ features in $CeIr_2$ are much stronger than those in γ-cerium. It is possible, in principle, to fit these spectra to a sum of individual peaks, determine area ratios, and then quantitatively estimate the valence by comparison to model calculations.[11] In our results, the background and the individual line shape changed as the coverage increased, making such quantitative fits unreliable. In this paper we are primarily interested in qualitative trends in the valence, from trivalence to weak mixed valence to strong mixed valence, so that quantitative estimation of the valence is not necessary. We will use the term "γ-like" to refer to spectra exhibiting weak mixed valence comparable to γ cerium, and "α-like" to refer to spectra with strong mixed valence comparable to $CeIr_2$.

Figure 4 shows the Ce $3d$ spectra for the Ce/Re system. Only $4f^1$ final-state peaks are observed at and below 0.6 ML, indicating that Ce is trivalent for these coverages (of course, a small degree of mixed valence cannot be excluded, given the statistics). The $4f^0$ and $4f^2$ features appear at coverages greater than 1 ML. As the cerium coverage increases from 1.0 to 2.0 ML, these features grow relatively larger. At 4.7 ML, they become broader, and the line shape becomes γ-like.

Figures 5 and 6 show the Ce $3d$ spectra for the Ce/Ir and Ce/Pt systems, respectively. In the Ce/Ir case, the cerium appears to be trivalent at and below 0.25 ML. Above 0.4 ML, $4f^0$ and $4f^2$ features appear and grow stronger with increasing coverage. The line shapes between 0.4 and 4.0 are α-like or strongly mixed valent. For the Ce/Pt system in Fig. 5, the growth pattern is similar to the Ce/Ir system: Ce is trivalent at low coverages, and mixed valent above 0.5 ML. Careful comparison to Fig. 4 shows that the line shapes at higher coverages, where the mixed-valent features exist, are different from those in the Ce/Re system.

We compare the M $4f$ spectra of clean substrates to those with Ce overlayers in Fig. 7. In the Ce/Re system,

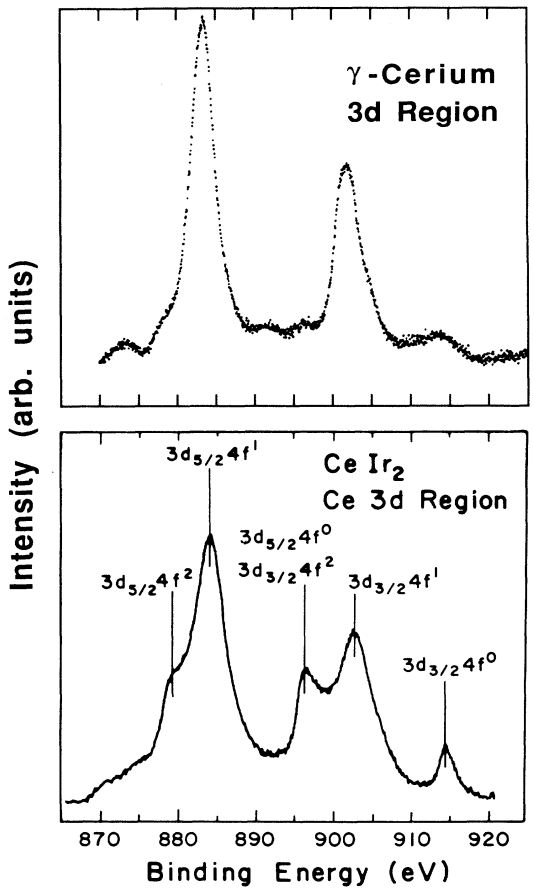

FIG. 3. Ce $3d$ region of γ-cerium (upper) and $CeIr_2$ (lower). The $CeIr_2$ spectrum is reproduced from Ref. 16, and the peaks are labeled according to spin-orbit splittings and final states. It is clear that $CeIr_2$ (α-like cerium compound) has much stronger $4f^1$ and $4f^2$ features, and the $4f^1$ binding-energy values (884.5 and 902.9 eV) are higher than those of γ-cerium (883.5 and 901.8 eV).

no binding-energy shift of the Re $4f$ was observed at any coverage. In the Ce/Ir system, no obvious shift at coverages lower than 1.0 ML was seen, but when going from lower to higher coverages, a gradual shift towards smaller binding energy was observed, reaching a value of 0.5 eV at 4.7 ML. In the Ce/Pt system, a shift towards higher binding energy of 0.1 eV was already observed at 0.5 ML, and at 2.55 ML this became 0.2 eV. The implication of these shifts will be discussed later.

The effect of annealing has also been studied. Figure 8 compares Ce $3d$ spectra for unannealed and annealed films for all three systems. The coverages displayed in the figure are chosen as the "critical coverages" where $4f^0$ and $4f^2$ spectra start to show up in each system. For Ce/Re no change is observed on annealing, while in both Ce/Ir and Ce/Pt the mixed-valence feature was enhanced after annealing. The changes in the Ce substrate count rate ratio (i.e., average stoichiometry) after annealing were also recorded for different initial coverages. There were no changes in the Ce/Re system. At lower coverages where the cerium shows only trivalent features, there was no significant change in the Ce/Ir or Ce/Pt system. At higher coverages of Ce/Ir and Ce/Pt, where mixed-valent features occur, we found that the Ce-substrate count rate ratio decreases in both systems, and that the Ce-Pt ratio drops faster than the Ce-Ir ratio under the same annealing conditions.

In Fig. 9 we plot the Ce $3d_{3/2}$ binding energy (determined for the $4f^1$ final state) versus coverage. The dashed line in this plot represents the $3d_{3/2}$ binding energy (901.8 eV) for γ-cerium. At low coverages the binding energies are similar for all three systems, but as the coverage increases the shift is quite different. In Ce/Re, at critical coverage (1.0 ML) for the onset of mixed valence the binding energy is fairly close to that of γ-cerium. In comparison, Ce/Ir and Ce/Pt have higher binding energies at the respective critical coverages (0.4 and 0.5 ML) and the binding energy does not approach the γ-cerium value as rapidly as in the Ce/Re system.

IV. DISCUSSION

A. General comments

Before proceeding we first wish to offer some general comments on the use of Ce $3d$ or M $4f$ binding energies and line shapes, as well as changes in the adsorbate-substrate count rates, in order to infer the mode of

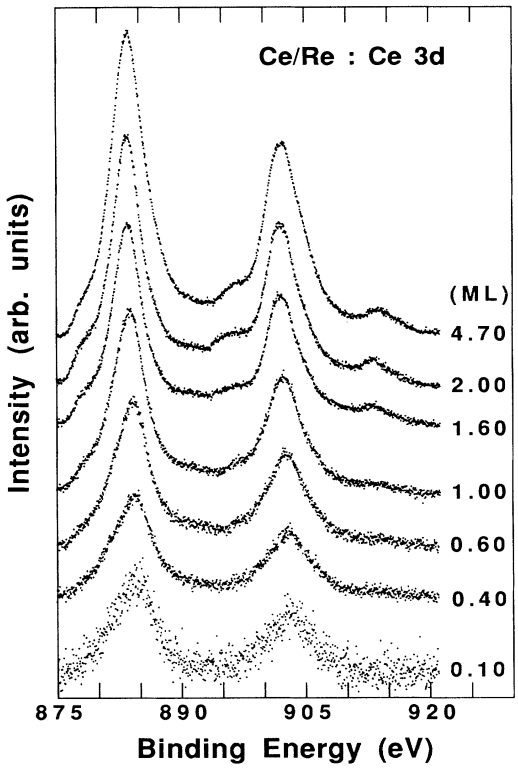

FIG. 4. Ce $3d$ region of the Ce/Re system for the following Ce coverages (in ML): 0.1; 0.4; 0.6; 1.0; 1.6; 2.0; 4.7. Note that below 0.6 ML only trivalent ($4f^1$) features exist, and the $4f^0$ features at 915 eV start to show up at about 1.0 ML. Curves at different coverages are scaled to show details (as are those in the Ce/Ir and Ce/Pt systems in Figs. 5 and 6).

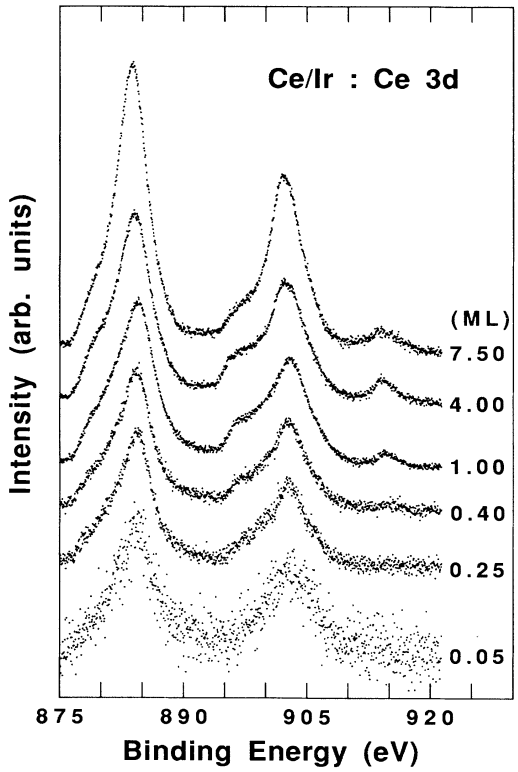

FIG. 5. Ce $3d$ region of the Ce/Ir system for the following Ce coverages (in ML): 0.05; 0.25; 0.4; 1.0; 4.0; 7.5. Note that at the lowest coverages, 0.05 and 0.25 ML, Ce is trivalent. The mixed-valent features appear at 0.4 ML, and are strongest between 1.0 and 4.0 ML. As more Ce is deposited (7.5 ML), the spectra become γ-like. As mentioned in the text, coverages are calculated from nonreactive models, and the actual Ce amount is higher than indicated.

growth of cerium films on the different substrates. Clearly, in the absence of low-energy electron diffraction or scanning tunneling microscopy studies on single-crystal surfaces, such information is limited. Nonetheless, some implications can be drawn.

First of all, observation of a binding-energy shift of the M $4f$ level clearly implies a reaction with Ce. However, because the XPS probing depth is substantially larger than a monolayer, it follows that when interdiffusion is weak or absent the substrate binding-energy shift at low coverages (i.e., for the first layer of substrate) is hard to observe because only the outer substrate layer reacts with the Ce so that shift is "averaged out" by the majority of unreacted underlayers. Unambiguous observation of a binding-energy shift occurs either when the range of interdiffusion is greater than or comparable to the probing depth, or at higher coverages of cerium when the only substrate atoms contributing to the XPS spectra are those right at the interface.

The Ce $3d$ spectra can be used in two ways. First, the Ce valence, as reflected in the line shape, is a function of environment. Studies[2] of submonolayer films of Ce on the refractory substrate W(110) show that the Ce valence varies smoothly with coverage; Ce is more weakly mixed valent than γ-cerium at 0.5 ML and more strongly mixed valent than α-cerium at 1.0 ML. The valence would have to decrease again beyond 1 ML, since in thicker layers or islands of cerium the valence should be that of γ-cerium. For reactive substrates there are other possibilities. In cases where M may form strongly mixed-valent bulk compounds with cerium, e.g., $CeIr_2$, a large cerium valence can indicate reaction. For substrates forming trivalent Ce compounds, a value of valence smaller than the γ-Ce value can indicate reaction. Clearly, valence alone cannot determine the exact cerium environment, but it can be used as part of an overall argument.

The Ce $3d$ binding energy is also sensitive to environment. For example, in Fig. 3 it can be seen that the binding energy of the $4f^1$ feature is more than 1 eV larger in $CeIr_2$ than in γ cerium. To emphasize this we plot in

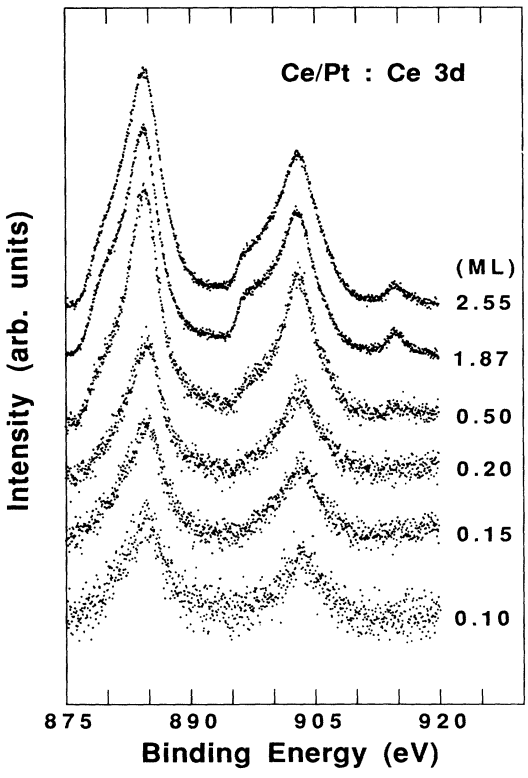

FIG. 6. Ce $3d$ region of the Ce/Pt system for the following Ce coverages (in ML): 0.1; 0.15; 0.2; 0.5; 1.87; 2.55. The mixed-valent feature appears at 0.5 ML; below that coverage Ce has trivalent features.

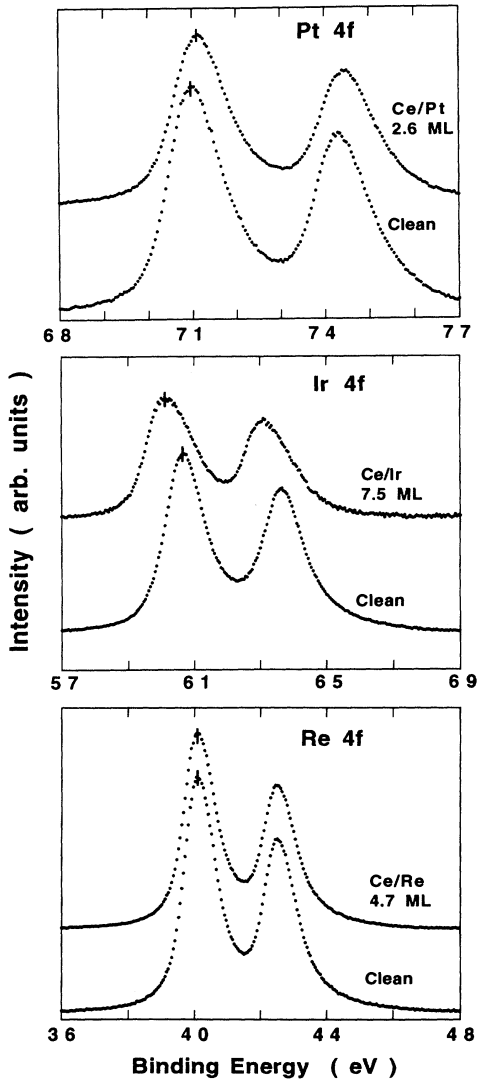

FIG. 7. Transition-metal $4f$ spectra. Comparison between clean substrates (lower curve in each frame) and those covered with Ce (upper curve in each frame) is provided. For Ce/Re, $\theta=4.7$ ML, no binding-energy shift is observed. For Ce/Ir, $\theta=7.5$ ML, a shift of 0.5 eV to lower binding energy is observed. For Ce/Pt, $\theta=2.55$ ML, a shift of 0.2 eV to higher binding energy is observed.

Fig. 9(b) data of Ref. 11 for the $3d_{3/2}$ binding energy as a function of composition x for Ce_xNi_{1-x} intermetallic compounds. The binding energy decreases as the Ce percentage increases towards pure cerium. Other Ce transition-metal compounds, whether γ-like or α-like, also have higher Ce $3d$ binding energies than γ-cerium.[11] The observation of a lower binding energy means the cerium atoms are surrounded primarily by cerium nearest neighbors, while higher binding energies can represent some degree of Ce-M reaction, but do not distinguish Ce at the surface from Ce surrounded by a specific M intermetallic coordination. Because the binding-energy values we observe are actually the "averaged" values from the probing depth region where a Ce concentration gradient may exist, the observation of a certain binding-energy value does not provide exact information about the compound stoichiometry or morphology. Nonetheless, we can still determine whether Ce is in a Ce-rich environment (binding-energy values closer to that of γ-cerium) or in M-rich environment (Ce compound with higher binding-energy values).

Annealing will promote diffusion and formation of stable compound phases in the case of strong Ce-substrate interaction. In a nonreactive case, however, binding energies, adsorbate-substrate count rate ratios, and/or line shapes should be unaffected by annealing.

B. Ce/Re

In Fig. 4, it can be seen that Ce is trivalent at low coverages from 0.1 up to 1.0 ML. Above 1.0 ML $4f^0$ and $4f^2$ peaks appear, and finally the line shape approaches that of γ-cerium as the cerium film thickens. The curve

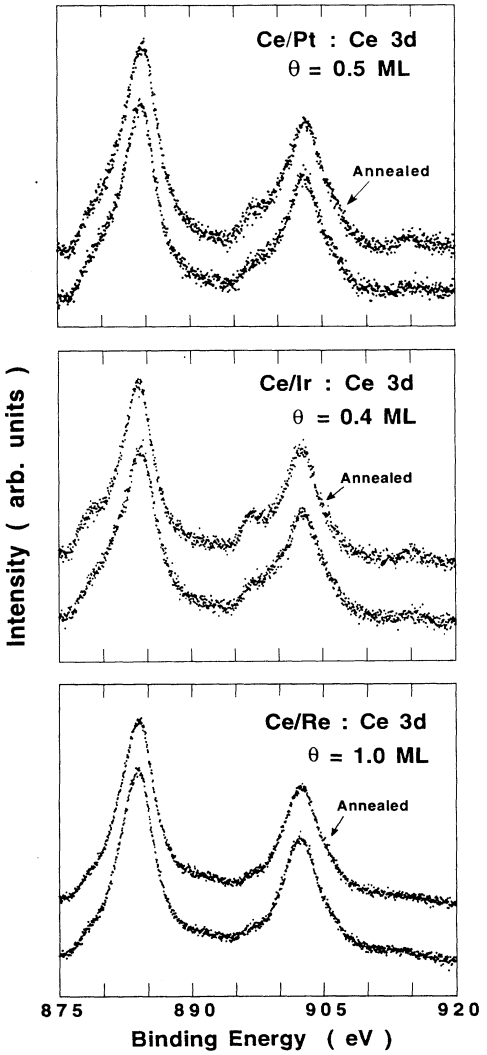

FIG. 8. Comparison of the Ce $3d$ spectra between unannealed and annealed Ce/M films. The coverage displayed is the "critical" coverage where mixed valency first appears. Note that in Ce/Pt and Ce/Ir the annealed spectra show enhanced mixed-valent features after annealing.

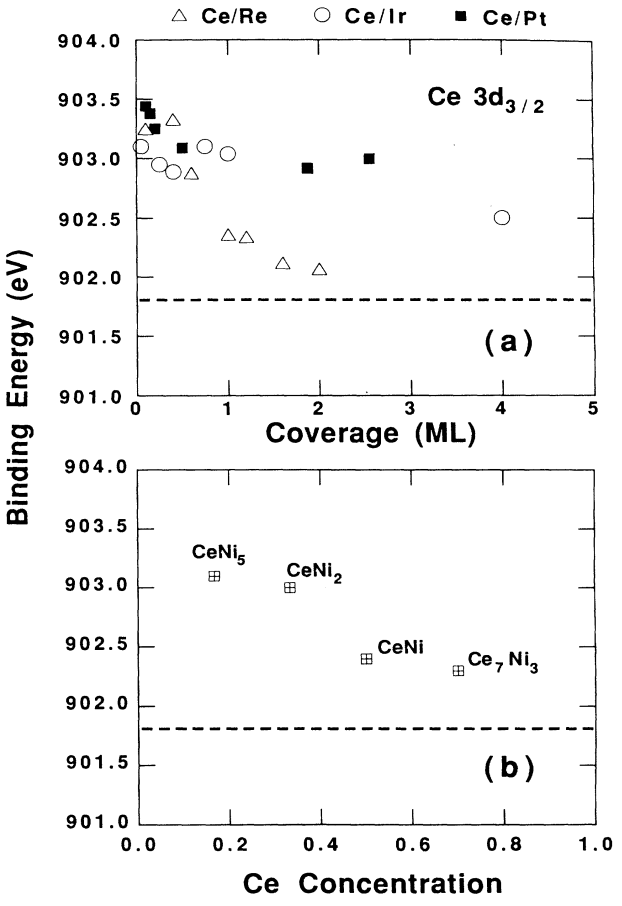

FIG. 9. (a) Ce $3d_{3/2}$ binding energies vs coverage for all three systems. The dashed line indicates the γ-cerium value (901.8 eV). Note that the Ce/Re curve approaches the γ-Ce value much faster than the other two. (b) Binding energy of the Ce $3d_{3/2}$ peak vs Ce concentration in Ce_xNi_{1-x} compounds. The compounds included are the following: $CeNi_5$, $x=0.17$; $CeNi_2$, $x=0.33$; CeNi, 0.5, Ce_7Ni_3; $x=0.7$. Data are obtained from Ref. 11. The γ-cerium value is indicated by the dashed line. Clearly, as the Ce concentration increases, the binding energy shifts towards a lower value.

for 2.0 ML seems to indicate a value of mixed valence slightly larger than that of γ-Ce. We do not think this behavior is due to Ce/Re alloying, for several reasons. First, as mentioned in the Introduction, no bulk Ce/Re intermetallics are stable. Second, Fig. 7 shows that there is no Re $4f$ binding-energy shift at any coverage below 4.7 ML. Third, the Ce $3d$ binding energy at 2.0 ML (Fig. 9) is already very close to that of γ cerium. Fourth, we have also annealed the Ce/Re film at 1.0 ML, where the mixed-valent $4f^0$ feature first appears. No significant changes in the line shape, binding energy, or count rate ratio were found on annealing. This result (no changes on annealing) is quite different from the behavior on annealing of Ce/Pt and Ce/Ir (see Fig. 8). Considering the above evidence, we conclude that Ce grows without intermixing on the Re surface, and the origin of the mixed-valent line shapes at higher coverages must be due to cerium-cerium interaction, i.e., formation of γ-cerium.

In the Ce/W(110) system studied by Gu *et al.*,[2] the relative heights of peaks in the valence band at 2 eV and the Fermi level were used as an indication of valence. The Ce valence-band feature goes from γ-like (at less than 0.5 ML) to α-like (at around 0.87 ML), and then back to γ-like above 1 ML, and at 1.0 ML the Ce-Ce lattice constant is 2% less than that of α-cerium. It is plausible that the line shapes between 1.0 and 2.0 ML in Ce/Re reflect a similar phenomena, i.e., contraction of the lattice constant of the ultrathin Ce film to values smaller than that of the stable γ phase, with concomitant higher valence, followed by the return to γ-like behavior at higher coverage.

C. Ce/Ir

In Fig. 5, it can be seen that the cerium $3d$ region exhibits trivalent features below 0.4 ML. At 0.4 ML, mixed valency first appears; it grows stronger up to about 4.0 ML. Finally, as more cerium is deposited, the region being probed becomes cerium rich, and the Ce line shape at 7.5 mL becomes more γ-like.

The mixed-valent line shape at 4.0 ML closely resembles that of $CeIr_2$; both have strong $4f^0$ and $4f^2$ peaks. The binding energy at 4.0 ML is also very close to that of $CeIr_2$. Together with the binding-energy shift, discussed next, we take this as evidence that Ce-Ir interaction is the origin of the mixed-valent line shape, as opposed to Ce-Ce interaction as in the Ce/Re system. (Observation of a line shape essentially identical to that of $CeIr_2$ does not necessarily imply that the latter compound forms at the surface. Indeed we expect some variation of stoichiometry, since the film should be Ce rich in the outer layers, and Ir rich in the inner layers. The observed line shape averages over this region; the strong mixed valence arises from Ce atoms surrounded by several Ir atoms.)

There was no significant Ir $4f$ binding-energy shift at low coverages from 0.05 to 1.0 ML. A shift of 0.2 eV appears at 4.0 ML, and a shift of 0.5 eV was observed at 7.5 ML. We annealed at 0.05, 0.4, and 1.0 ML in order to see whether strong mixed valence, which represents strong Ce-substrate interaction, would appear. No significant change was observed at 0.05 ML, but we did see enhancement of $4f^0$ and $4f^2$ peaks at 0.4 and 1.0 ML, while the Ce-Ir count rate ratio remained constant. This means that the Ce-Ir interaction was promoted by annealing. Sequential annealings were performed on a higher coverage (1.2 ML) film; a weak enhancement of mixed valence and a non-negligible decrease of the Ce-Ir count rate ratio were observed.

While these observations make clear that Ce-Ir interactions and interdiffusion are important, two facts suggest that interdiffusion is weak at room temperature. The first is that the Ir $4f$ binding-energy shift does not occur below 1 ML. The second is the fact that the valence increases after annealing; it requires a temperature greater than 300 K to promote the diffusion which allows for strong Ce-Ir interaction.

D. Ce/Pt

Ce/Pt has a very similar growth pattern to that of the Ce/Ir system, i.e., Ce is trivalent at low coverages and mixed valent at higher coverages. The onset of mixed-valent features occurs near 0.5 ML.

A shift of the Pt $4f$ of 0.1 eV towards higher binding energy can be seen at 0.5 ML (compared to Ce/Ir where no Ir $4f$ shift is seen below 1 ML) and a shift of 0.2 eV at 2.55 ML was observed. This implies that even with a small deposition of deposited Ce, interdiffusion is sufficiently strong at room temperature to render the substrate binding-energy shift visible.

No change in the Ce $3d$ line shape for 0.1 ML was observed on annealing. Enhancement of mixed valence was observed for 0.5 ML but for 1.87 ML the mixed valence appears to weaken somewhat on annealing. The Ce $3d$ binding energies remain large in Ce/Pt and approach the γ-Ce value slowly, which suggests that a Ce/Pt mixed layer forms as opposed to growth of a γ-Ce film. Taken together, these facts suggest that for Ce/Pt reaction is important, and that interdiffusion is stronger than for Ir substrates.

E. Comparison of the three cases

At the lowest coverages Ce is trivalent on all three substrates. This suggests that an isolated Ce atom on the surface of a transition metal will be trivalent. This is consistent with a larger body of work showing that the lower valence state tends to be stable at surfaces, just as in the free atom.[19] A further common feature is that there appears to be a threshold near 0.5 ML below which Ce is trivalent and above which it becomes mixed valent. This threshold could represent either the onset of Ce clusters (with valence close to γ-Ce) or the beginning of mixed-valent Ce/M compound formation.

The Ce $3d$ binding energies are similar for all three systems at low coverage, and similar to values reported by Fuggle *et al.*[11] for various Ce/M intermetallics, but more than an electron volt greater than that of γ-Ce. Apparently the Ce-Ce bond does a better job of screening the Ce $3d$ core hole than does the Ce-M bond. The case of Ce/Re, where reaction is weak, suggests that the high binding energy at the surface does not arise from charge

transfer from Ce to Re, but is caused by poor screening at the surface. The three compounds also show different trends of the $3d$ binding energy as coverage increases. For Ce/Ir and Ce/Pt the binding energies remain large and decrease gradually, due to interdiffusion and reaction. (It is possible that, in addition to final-state screening, differences in the Ce $4f$ initial-state wave function due to strong mixed valence contribute to the large $3d$ binding energy in Ce/Ir and Ce/Pt.)

In the case of Ce/Pt the Pt $4f$ already exhibits a binding-energy shift at coverages as low as 0.5 ML. This suggests stronger reaction and/or interdiffusion at room temperature than for the other substrates, where M $4f$ shifts were not observed at such low coverages. For Ce/Ir a $4f$ binding-energy shift was observed at higher coverages. For Ce/Re no shift was observed at any coverage. According to the report on work in the Ce/W(110) system,[2] a surface W $4f$ energy shift at low coverages was observed with surface-sensitive (low photon energy) photoemission; as the Ce coverage increased the shift disappeared. As discussed in Sec. IV A, at low coverages the Re surface layer forms such a small fraction of the Re atoms within the XPS probing depth that such a $4f$ shift for the surface atoms would be difficult to observe and cannot be ruled out.

The morphology of overlayer growth depends on both surface energies (surface tensions) and energy of compound formation;[9] the higher the substrate surface energy compared to that of the adsorbates, the more epitaxial the growth pattern. When the surface energies of both substrate and adsorbate are similar, interdiffusion is favored. Both Re and Ir have high surface energies for metals, while Pt has a lower value that is closer to that of Ce than either Re or Ir.[20–22] Ce-Re compounds are not energetically favored, while the other two M do form a series of stable compounds with cerium.[10] The interplay between these two factors can be seen very clearly here. Ce/Re growth is very likely epitaxial, since neither interdiffusion nor interaction is favored. For Ce/Ir interaction is favored but not interdiffusion, while for Ce/Pt both are expected; this is consistent with our observation that interaction occurs for both cases but that diffusion is stronger in the latter case. Our preliminary measurements for Ce/Au (which has been previously studied by Raaen[8]) show that the interdiffusion is stronger at room temperature than for any of Re, Pt, or Ir. This is consistent with the fact that Au has a lower surface energy, relatively close to that of Ce.

We have also noticed that the M $4f$ binding-energy shifts at higher coverages are different for different substrates: the Ir $4f$ is shifted by 0.5 eV to lower binding energy, the Pt $4f$ is shifted 0.2-eV higher, while the Au $4f$ (as reported in either Ref. 8 or seen in our preliminary experiments) shows a shift of 0.5 to 1.0 eV to higher values. In Ref. 9, the authors explain the shifts of Cu $3d$ and Au $4f$ binding energies toward higher values as the effect of f-conduction-band hybridization, by which the d-electron screening of the core hole is reduced. In Ce/Ir, where f-conduction-band hybridization is stronger than for either Ce/Cu or Ce/Au, we observed a significant shift toward the *lower* binding energy. We also have observed a smaller positive binding-energy shift in the Ce/Pt system, where mixed valency (or strong hybridization) is also present (Fig. 6). Hence, the binding-energy shift can be either positive or negative. We thus believe that a systematic explanation for such binding-energy shifts is more complicated than suggested in Ref. 9.

ACKNOWLEDGMENTS

This work was supported in part by funds from the Research Corporation (Award Number R-164), and by the Institute for Surface and Interface Science at UCI.

[1]H. Homma, K.-Y. Yang, and I. K. Schuller, Phys. Rev. B **36**, 9435 (1987).

[2]C. Gu, X. Wu, C. G. Olson, and D. W. Lynch, Phys. Rev. Lett. **67**, 1622 (1991).

[3]N. A. Braaten, J. K. Grapsted, and S. Raaen, Phys. Rev. B **40**, 7969 (1989).

[4]M. Grioni, J. Joyce, S. A. Chambers, D. G. O'Neill, M. del Giudice, and J. H. Weaver, Phys. Rev. Lett. **53**, 2331 (1984).

[5]A. Fujimori, M. Grioni, J. J. Joyce, and J. H. Weaver, Phys. Rev. B **36**, 1075 (1987).

[6]F. U. Hillebrecht, Appl. Phys. Lett. **55**, 227 (1989).

[7]S. Raaen, N. A. Braaten, J. K. Grepstad, and S. L. Qiu, Phys. Scripta **41**, 1001 (1990).

[8]S. Raaen, Solid State Commun. **73**, 389 (1990).

[9]S. Raaen, C. Berg, and N. A. Braaten, Surf. Sci. **269/270**, 953 (1992).

[10]See, e.g., W. G. Moffatt, *The Handbook of Binary Phase Diagram, Ce Compounds* (Genium, New York, 1984).

[11]J. C. Fuggle, F. U. Hillebrecht, Z. Zolnierek, R. Lasser, Ch. Freiburg, O. Gunnarsson, and K. Schonhammer, Phys. Rev. B **27**, 7330 (1983).

[12]M. Campanga and F. U. Hillebrecht, in *Handbook of the Physics and Chemistry of Rare Earths,* edited by K. A. Gshneidner, Jr., L. Eyring, and S. Hufner (North-Holland, New York, 1987), Vol. 10, Chap. 63.

[13]G. Ertl and J. Kuppers, *Low Energy Electrons and Surface Chemistry,* 2nd ed., (VCH, Deerfield Beach, FL, 1985), pp. 74–79.

[14]C. S. Hemminger (private communication). These sensitivity factors are relative to F 1s sensitivity factor of 1.0.

[15]A. Zangwill, *Physics at Surfaces* (Cambridge University Press, Cambridge, 1988), pp. 21.

[16]J. M. Linquist, J. C. Hemminger, and J. M. Lawrence, Phys. Rev. B **36**, 5819 (1987).

[17]N. A. Braaten, J. K. Grepstad, and S. Raaen, Surf. Sci. **222**, 499 (1989).

[18]J. W. Allen, S. J. Oh, O. Gunnarsson, K. Schonhammer, M. B. Maple, S. Torikachvili, and I. Lindau, Adv. Phys. **35**, 275 (1986).

[19]A. Zangwill, in *Giant Resonances in Atoms, Molecules, and Solids,* edited by J. P. Connerade, J. M. Esteva, and R. C. Karnatak (Plenum, New York, 1987), pp. 332–333.

[20]R. J. Needs, M. J. Godfrey, and M. Mansfield, Surf. Sci. **242**, 215 (1991).

[21]A. R. Miedema, in *Physics of Transition Metals 1980,* edited by P. Rhodes (The Institute of Physics, Bristol, 1981), pp. 413. The heat of evaporation is proportional to surface energy and thus can provide relative values for Re, Ir, Pt, Au, and Ce.

[22]L. Z. Mezey and J. Giber, Jpn. J. Appl. Phys. **21**, 1569 (1982).